

# Aerodynamic Analysis of Diffuser with Airfoil-Based Curved Geometry Across Various Prototypes

Journal of Mechanical Engineering,  
Science, and Innovation  
e-ISSN: 2776-3536  
2025, Vol. 5, No. 1  
DOI: 10.31284/j.jmesi.2025.v5i1.7313  
ejurnal.itats.ac.id/jmesi

**Galang Baruna Ramadhan<sup>1</sup>, I Kade Wiratama<sup>1</sup>, and I Wayan Joniarta<sup>1</sup>**

<sup>1</sup>Department of Mechanical Engineering, Faculty of Engineering, University of Mataram, Indonesia

**Corresponding author:**

I Kade Wiratama

Department of Mechanical Engineering, Faculty of Engineering, University of Mataram, Indonesia

Email: kwiratama@unram.ac.id

## Abstract

*The diffuser can increase air velocity in wind turbines by utilizing pressure differences, particularly in small-scale wind turbines. However, some previous research still uses a simple diffuser shape. One alternative diffuser shape is using the airfoil, the Wortmann Fx 63-137 airfoil has high lift, exhibits soft stall characteristics, and has excellent overall performance. This study aims to analyze the wind velocity and wind power output generated by an airfoil-based diffuser. Aerodynamic simulations were used with an inlet wind speed of 5.6 m/s. The diffuser has a diameter of 1020 mm, with length to diameter ratios of 0.1, 0.137, 0.221, and 0.371, with angles of attack from 0° to 8° in 2° increments. The results show that the diffuser 0.371 ratio at an 8° angle of attack achieved the highest wind speed of 10.22 m/s, it generate 513 watts. Conversely, the lowest wind speed was observed with a 0.1 ratio at an 8° angle, where the velocity reached 6.58 m/s, producing 137 watts of wind power. Those findings indicate that diffuser length is directly proportional to wind velocity. However, variation in the angle of attack result in maximum wind velocity at specific angles, and wind power output is directly proportional to wind velocity.*

**Keywords:** Wortmann FX63-137 Airfoil; Diffuser; Wind Power; Wind Speed

Received: February 10, 2025; Received in revised: March 27, 2025; Accepted: April 10, 2025

Handling Editor: Ayu Setyaning Poesoko

## INTRODUCTION

Wind energy originates from the movement of air and temperature changes on the surface of land and sea. Generally, wind speed varies depending on topography, geography, and season [1]. Wind energy is considered a clean and environmentally friendly energy source because it does not produce carbon dioxide (CO<sub>2</sub>), and wind does not generate harmful waste for the environment [2]. One of the technologies used to convert wind energy into mechanical energy is wind turbines, which have been widely



Creative Commons CC BY-NC 4.0: This article is distributed under the terms of the Creative Commons Attribution 4.0 License (<http://www.creativecommons.org/licenses/by-nc/4.0/>) which permits any use, reproduction and distribution of the work without further permission provided the original work is attributed as specified on the Open Access pages. ©2025 The Author(s).

implemented in various regions to generate electricity (wind farms) [3], [4], as well as for other needs. The design of wind turbines heavily considers the aerodynamic aspects of their blades to achieve optimal aerodynamic performance [5]. However, for modern wind turbines, the focus is not only on blade aerodynamics but also on enhancing the available wind energy. One way to achieve this is by incorporating a diffuser into the wind turbine system [6]. Therefore, to increase the power output of wind turbines, especially in small-scale applications, DAWT (Diffuser Augmented Wind Turbine) technology, also known as Wind Lens, is utilized [7].

The operating of Diffuser Augmented Wind Turbine (DAWT) is based on the principle of creating a pressure difference between the outer and inner sections of the diffuser [8]. Essentially, a diffuser is an aerodynamic funnel-shaped structure designed to enhance the power output of a wind turbine by utilizing the air that flows into it. This is achieved through the pressure difference, which creates a suction effect [9]. Wind turbines equipped with diffusers can significantly increase wind speed [10]. Among the various diffuser designs, the airfoil-shaped diffuser has garnered considerable attention due to the numerous possibilities it offers researchers [11].

The airfoil design creates lift, enhancing airflow through the diffuser [12]. This lift force is also utilized for various applications beyond diffusers, such as in wing and propeller designs [13]. Airfoil design has advanced significantly over time and has undergone numerous modifications. Generally, airfoils are optimized to reduce drag and increase lift. Most of these optimizations have been carried out numerically with the help of CFD (Computational Fluid Dynamics) simulations [14].

Research related to wind turbine diffusers has been conducted by Yuji Ohya and Takashi Karasudani [15], who investigated the power output generated by wind turbines equipped with a diffuser and an additional plate called a "Brim" at the rear. The Brim is designed to create a low-pressure area behind the diffuser. Ohya and Karasudani [15] used a ratio to evaluate the diffuser, specifically comparing the length of the diffuser to the diameter of its throat. The diffusers were divided into four types based on this ratio: Type C<sub>0</sub> with a ratio of 0.1, Type C<sub>i</sub> with a ratio of 0.137, Type C<sub>ii</sub> with a ratio of 0.221, and Type C<sub>iii</sub> with a ratio of 0.371. The results showed an increase in the rotational speed of the wind turbine due to the diffuser. The wind speed is directly proportional to the length of the diffuser; the longer the diffuser, the greater the wind speed increases [15]. With the same objective, research on diffusers was also conducted by Toshio Matsushima et al. [16]. Their study used a diffuser with a diameter of 1 meter and lengths ranging from 2 to 4 meters, tested at various angles of attack from 0 to 12 degrees. The findings indicated that increasing the length of the diffuser enhanced wind speed. However, as the angle of attack increased, wind speed improved 6 degrees but decreased to 8 and 12 degrees [16]. Despite these advancements, the research by Yuji Ohya et al. [15] and Toshio Matsushima et al. [16] was limited to simple diffuser designs. This study aims to investigate diffusers with airfoil geometry, exploring various length-to-diameter ratios and angles of attack to enhance performance.

Numerous studies have been conducted on Wind Lens/DAWT technology, with researchers such as Mithil et al. [17] and Koichi [18]. Several studies have also been conducted in Indonesia, contributing to the field, including research by Yeni Putri Andriyani and Ketut [19], Evi et al. [20], and Fatahul et al. [21]. Such research is essential to develop the potential of wind energy available in Indonesia. Therefore, the purpose of this study is to determine the wind velocity at the throat of the diffuser for various lengths and angles of attack using simulation methods with Ansys Fluent. The goal of this research is to determine the wind velocity levels and power output produced by different types of airfoil-based wind turbine diffusers.

## METHODS AND ANALYSIS

Ohya and Karasudani [15] investigated the effect of diffuser to its length on wind velocity. Their findings showed that diffuser length can increase incoming wind speed. In their study, the wind speed within the diffuser was analyzed with various length variations, as shown in Table 1, using a diameter of 1020 mm. On the other hand, research related to diffusers was also conducted by Toshio Matsushima et al.[16], who examined the influence of diffuser shape on wind speed. Their results demonstrated that the angle of attack significantly affects the wind velocity in the diffuser, with maximum speed increases of up to 1.7 times achieved using an optimal diffuser shape. In this study, the diffuser lengths from Ohya and Karasudani [15] were utilized, along with the angles of attack based on Toshio Matsushima et al.[16] research, while incorporating an airfoil-based design.

The airfoil shape used in this studied is the Wortmann FX63-137. As can be seen on Figure 1, its topology has a thickness ratio of 13.66% and a curvature of 5.79%. This airfoil has high lift, exhibits gentle stall characteristics, and has excellent overall performance as well as suitable to low Reynold Number[22]. So that this airfoil is suitable for use as a diffuser in low wind speed regions.

Autodesk Inventor was used to design the airfoil-based diffuser, while Ansys Fluent was utilized to simulate the airflow entering the diffuser. The diffuser's dimensions, specifically its length ( $L_t$ ), were divided into several types as outlined in Table 1, based on the diameter ( $D$ ) and the angle of attack ( $\alpha$ ), with the addition of a brim ( $h$ ) as shown in Figure 2. The independent variables in this study are the diffuser length ( $L_t$ ) and the angle of attack ( $\theta$ ), while the dependent variables are the wind velocity in the diffuser and the resulting output power.

Type C<sub>0</sub>, as shown in Figure 3 (a), features a diffuser with a diameter ( $D$ ) of 1020 mm and a ratio of 0,1, resulting in a length ( $L_t$ ) of 102 mm. The brim size ( $h$ ) is 153 mm, and the angle of attack ( $\alpha$ ) is varied from 0° to 8° in 2° increments.

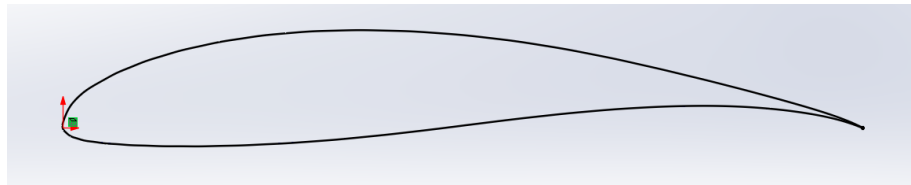


**Figure 1.** Profile Section Airfoil Wortmann FX 63-137

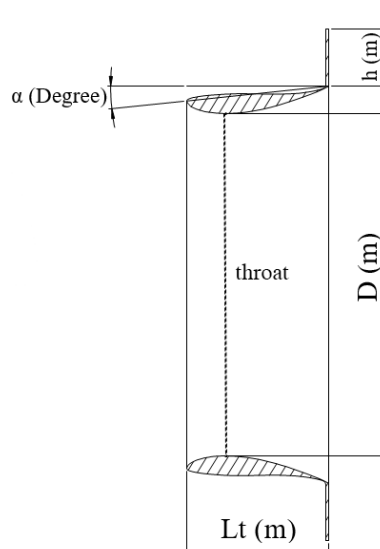


**Figure 2.** Airfoil Diffuser Parameters

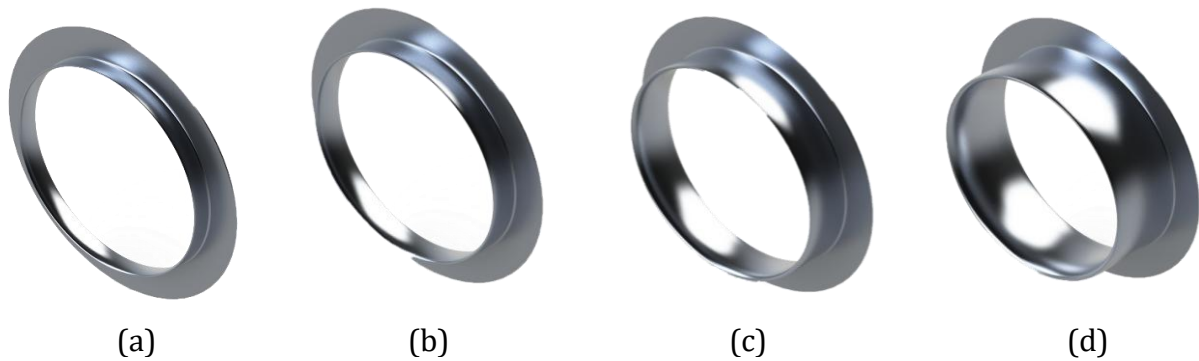


**Figure 3.** a) Diffuser type  $C_0$  with ratio 0,1  $L_t = 102$  mm, b) diffuser type  $C_i$  with ratio 0,137  $L_t = 139,74$  mm, c) diffuser type  $C_{ii}$  with ratio 0,221  $L_t = 225,42$  mm, d) diffuser type  $C_{iii}$  with ratio 0,371  $L_t = 378,42$  mm

**Table 1.** Types and Ratios of Airfoil Diffuser

No	Type of Diffuser	$L_t/D$
1	$C_0$	0,1
2	$C_i$	0,137
3	$C_{ii}$	0,221
4	$C_{iii}$	0,371

Type  $C_i$ , as shown in Figure 3 (b), uses the same diffuser diameter of 1020 mm but with a ratio of 0,137, giving it a length ( $L_t$ ) of 139,74 mm. The brim size ( $h$ ) remains constant at 153 mm, and the angle of attack ( $\alpha$ ) is also varied from  $0^\circ$  to  $8^\circ$  in  $2^\circ$  increments.

Type  $C_{ii}$ , as shown in Figure 3 (c), maintains the same diffuser diameter of 1020 mm but with a higher ratio of 0,221, resulting in a length ( $L_t$ ) of 225,42 mm. The brim size ( $h$ ) is 153 mm, and the angle of attack ( $\alpha$ ) is adjusted from  $0^\circ$  to  $8^\circ$  in  $2^\circ$  increments.

Type  $C_{iii}$ , as shown in Figure 3 (d), also has a diffuser diameter ( $D$ ) of 1020 mm but with a ratio of 0,371, leading to a length ( $L_t$ ) of 378,42 mm. The brim size ( $h$ ) remains at 153 mm, and the angle of attack ( $\alpha$ ) is varied from  $0^\circ$  to  $8^\circ$  in  $2^\circ$  increments.

### Geometry

The diffuser was designed using Autodesk Inventor Professional, with the dimensions outlined earlier. In Ansys Fluent, a domain and Boolean operation were used to enhance the simulation results. The size of the domain was based on the diameter of the diffuser ( $D$ ) 1020mm, with dimensions of  $12,5D \times 5D \times 3,5D$ , while the boolean operation was performed using a size of  $2\text{ m} \times 2\text{ m} \times 2\text{ m}$  [23], as illustrated in Figure 4.

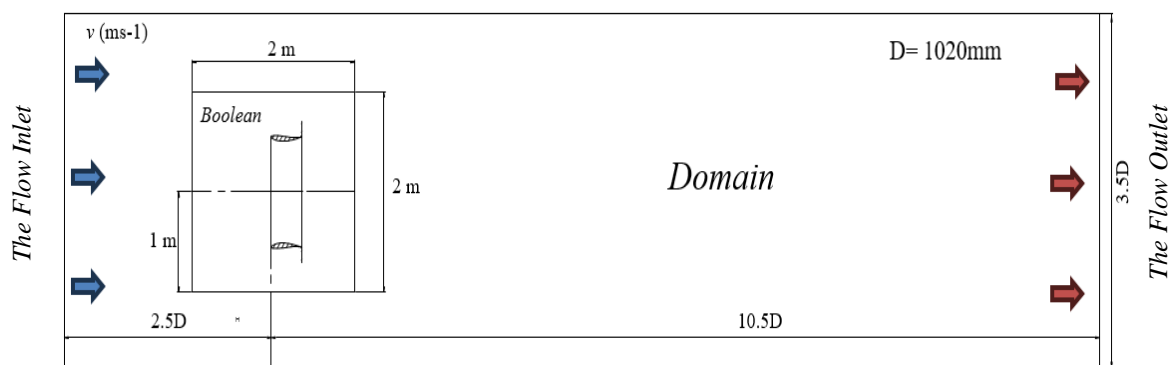


**Figure 4.** Domain and Boolean Size

The Boolean function is used to separate the mesh size between the domain and the Boolean region. The Boolean operation performed involves creating an empty space region as the target body, with the diffuser as the tool body[24]. The mesh size in the Boolean region is smaller than that in the domain, which serves to provide more detailed results in the diffuser area. The Boolean shape used is a cube with dimensions of 2 m x 2 m x 2 m.

### Meshing

Meshing is the process of dividing complex and continuous geometries into smaller areas, manageable elements [25]. In this case, we utilized a triangular cell mesh, as illustrated in Figure 5, with an element size of 500 mm. We set the curvature refinement with a minimum size of 3 mm and assigned a body size feature using the Body of Influence type, which had an element size of 300 mm. With these meshing settings, the total number of elements generated reached 1.5 million. Generally, a higher number of elements leads to more accurate simulation results [26].

To ensure a proper mesh setup, an independent test was conducted with varying numbers of elements to determine the accuracy level of the simulation based on the minimum error value [27]. The results used the average velocity values at the throat diffuser. A diffuser of type C<sub>ii</sub> with an angle of attack of 0 degrees was used for the Grid Independent Test (GIT). Those values were then compared until the smallest error obtained at a specific number of elements that was used for subsequent tests. The results of the independent test can be seen in Table 2.

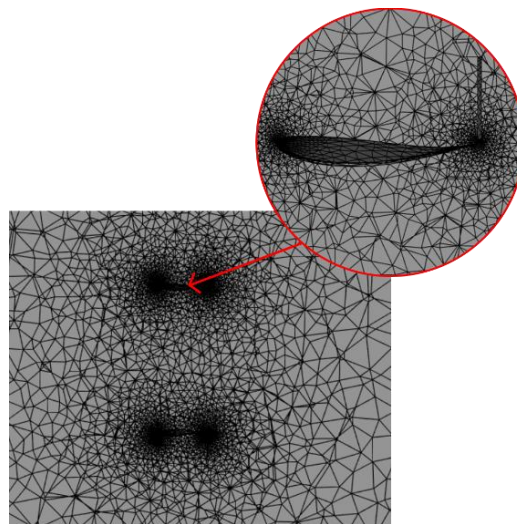


**Figure 5.** Meshing Results in Ansys Fluent

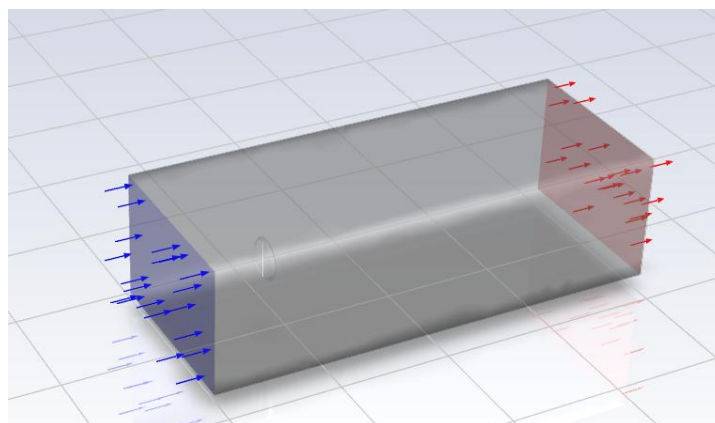


**Figure 6.** Boundary Condition

**Table 2.** The results of the Grit Independent Test (GIT)

No	Element	Velocity (m/s)	Error (%)
1	620473	8.251	2.32
2	740295	8.462	2.55
3	890733	8.421	0.48
4	1112953	8.431	0.15
5	1507878	8.443	0.106

### Boundary Condition

After completing the meshing process, the next step is the setup phase, which involves configuring the boundary conditions. Boundary conditions define the zones that limit the fluid system, ensuring the simulation aligns precisely with atmospheric conditions [28]. In this study, the fluid type for the domain is set to air by default (air density: 1,22 kg/m<sup>3</sup>). As shown in Figure 6, the inlet (blue) is assigned a wind velocity input of 5,6 m/s, based on the average wind velocity [29], while the outlet (red) is set to a pressure boundary condition of 0 Pa. The diffuser area and the domain wall are given no slip boundary conditions because the working fluid used is air. The viscosity is modeled using the K-Omega SST model (default)[30]. The simulation is then run for 250 iterations.

Based on Figure 2, the wind velocity data for the diffuser was obtained at the throat area, as the wind turbine is positioned in the throat section of the diffuser. The data collected from Ansys Fluent was processed using Microsoft Excel to determine the velocity and power generated for each diffuser variation. The power produced by the diffuser can be calculated using the equation (1) [21]:

$$P = \frac{1}{2} A \rho v^3 \quad (1)$$

Where,  $P$  is power,  $A$  is turbine swept area,  $\rho$  is air Density (1,225 kg/m<sup>3</sup>), and  $v$  is velocity

## RESULTS AND DISCUSSIONS

### Comparison of Velocity

The diffuser was tested at an wind speed of 5.6 m/s. For comparison, both an airfoil diffuser and a simple diffuser were simulated to evaluate the differences in wind speeds. All three diffusers had identical dimensions, with a constant ratio of  $C_i$  0,137 ( $Lt/D$ ) and an angle of attack ( $\alpha$ ) of 6 degrees. Data collection was performed at a distance 0,5 meters to the inlet and 0,5 meters from the inlet, measured at the center of the diffuser. The results are displayed in Figure 7.

According to Figure 7, the airfoil diffuser exhibits a higher wind speed than the simple diffuser. At the throat section, the airfoil diffuser achieves a velocity of 6.7 m/s, representing an increase of 19.64% from the initial speed (5.6 m/s), while the simple diffuser reaches a velocity of only 6,46 m/s, with an increase of 15.35% from the initial speed (5.6 m/s). This testing proves that using an airfoil on design diffuser enhances wind speed more effectively, even with the same diffuser dimensions. This improvement occurs because the airfoil creates a low-pressure region, which results in higher wind in that area.

### Wind Velocity

After comparing the airfoil-based and simple diffusers, the next step is to analyze the average wind speed at the throat area of the diffuser using Ansys Fluent. The results of the wind velocity analysis are displayed in Figure 8.

Based on Figure 8, the wind speed varies for each diffuser type, and increasing the



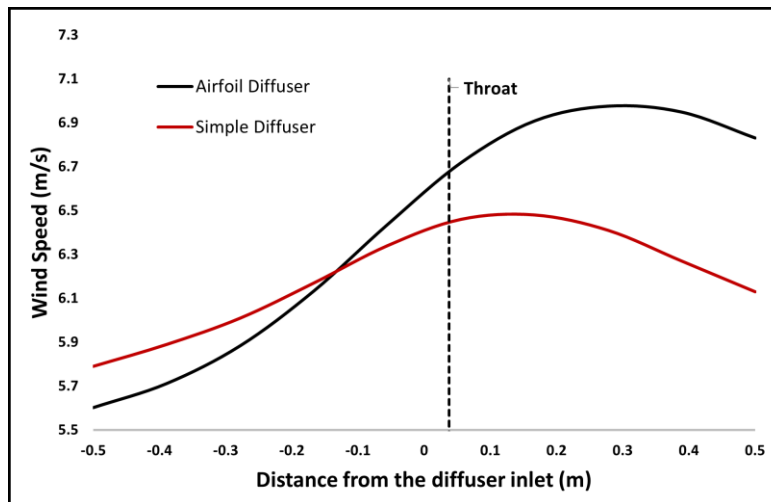


**Figure 7.** Comparison of wind speed between the airfoil diffuser and the simple diffuser

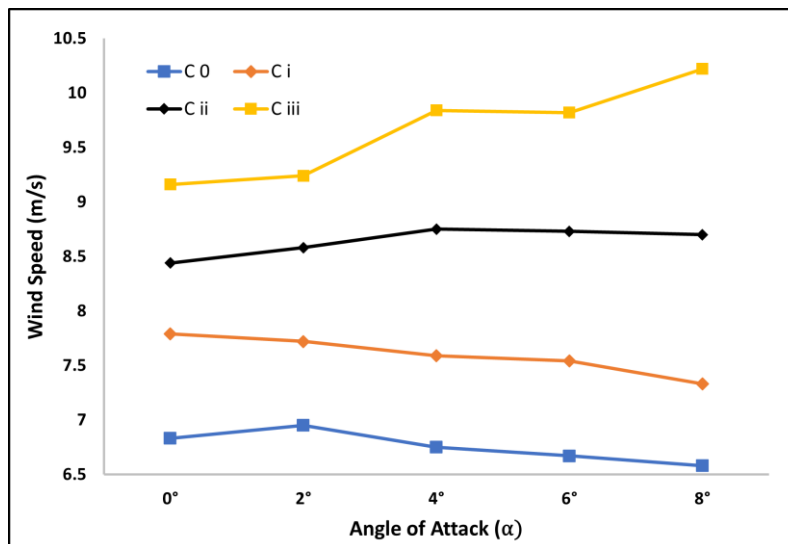
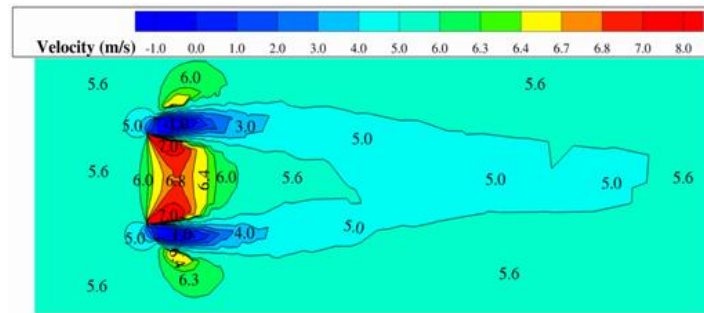


**Figure 8.** Wind speed at various angles of attack

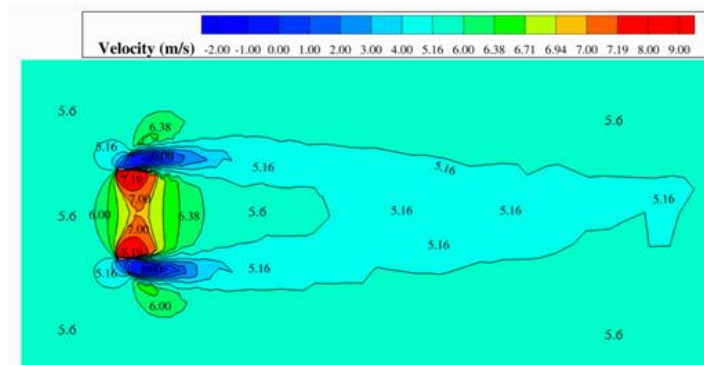
length of the diffuser enhances the wind speed. Type  $C_0$  has the lowest average wind speed among the other types, while Type  $C_{iii}$  has the highest average wind speed. Type  $C_0$  records an average wind speed of 6,75 m/s (increase 20,64% of wind speed), Type  $C_i$  records an average wind speed of 7,59 m/s (increase 35,61% of wind speed), Type  $C_{ii}$  records an average wind speed of 8,64 m/s (increase 54,29% of wind speed), and Type  $C_{iii}$  records an average wind speed of 9,65 m/s (increase 74,23% of wind speed). This aligns with the research by Ohya and Karasudani [15], which states that the length of the diffuser ( $L_t$ ) can influence the increase in wind speed.

However, variations in the angle of attack ( $\alpha$ ) result in fluctuations in wind velocity. Each type of diffuser reaches its maximum wind velocity at a different angle of attack. Type  $C_0$  achieves its peak wind velocity of 6,95 m/s at  $2^\circ$ , while Type  $C_i$  reaches its maximum wind velocity of 7,79 m/s at  $0^\circ$ . Type  $C_{ii}$  records its highest wind velocity of 8,75 m/s at  $4^\circ$ , and Type  $C_{iii}$  reaches a peak wind velocity of 10,22 m/s at  $8^\circ$ . These findings align with the research conducted by Toshio Matsushima et al. [16], which states that the angle of attack ( $\alpha$ ) significantly influences the wind velocity distribution within the diffuser, particularly in the throat area, as shown in Figure 8. The wind velocity is higher near the edges of the diffuser and lower in the center. This wind velocity distribution can enhance wind power available by utilizing the higher-speed airflow at the diffuser's edges to impact the turbine blades effectively. Additionally, the presence of a brim at the rear of the diffuser creates a low-pressure region, which further increases the airflow while it

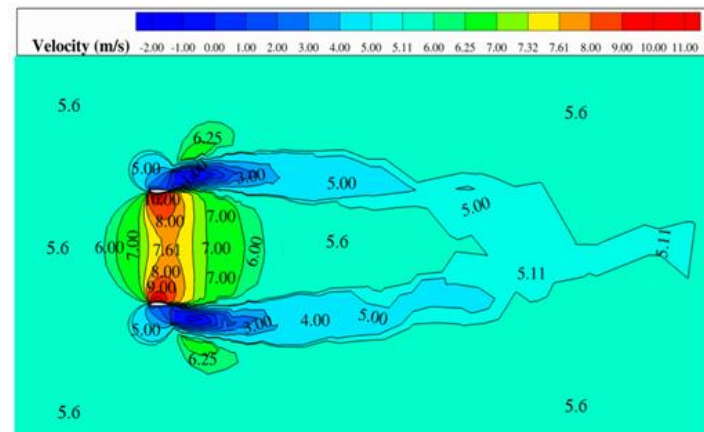
entering the diffuser.



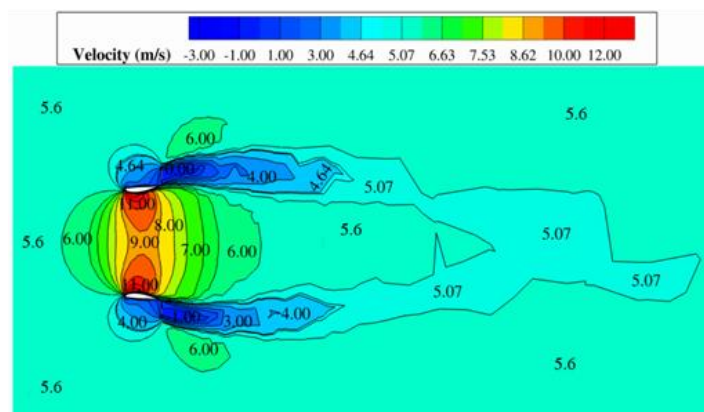
(a)



(b)



(c)



(d)

**Figure 9.** The highest wind velocity for each type based on the angle of attack, (a) Type  $C_0$   $2^\circ$  with ratio 0,1  $L_t=102$  mm, (b) Type  $C_i$   $0^\circ$  with ratio 0,137  $L_t=139,74$  mm, and (c) Type  $C_{ii}$   $4^\circ$  with ratio 0,221  $L_t=225,42$ , d) Type  $C_{iii}$   $8^\circ$  with ratio 0,371  $L_t=378,42$



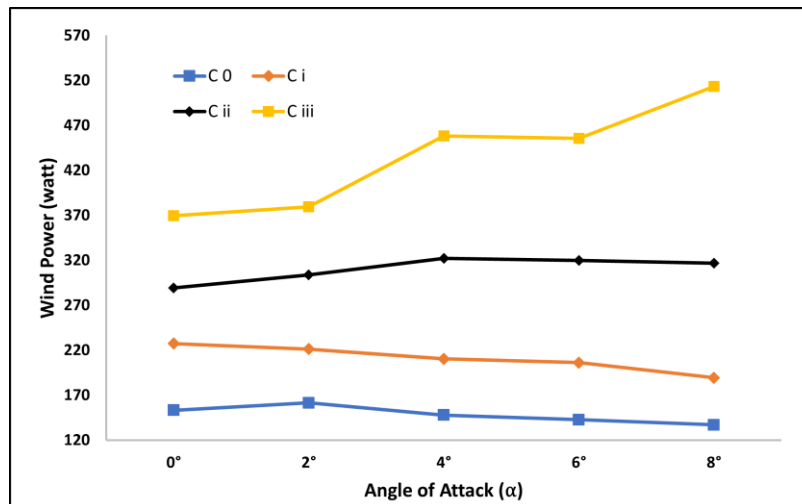


**Figure 10.** The wind power generated by each type of diffuser

### Output Wind Power

Wind speed is directly proportional to the wind power generated; the greater the wind speed, the higher the wind power output. With an incoming wind velocity of 5.6 m/s, the diffuser's output wind power increases noticeably, particularly at the throat section. The generated wind power available can be observed in Figure 10 below.

Based on the graph in Figure 10, which illustrates the relationship between wind power percentage and the angle of attack ( $\alpha$ ), a significant increase in wind power occurs at specific angles for each diffuser type. Diffuser type C<sub>0</sub> achieves a maximum wind power of 161 watts at a 2° angle, type C<sub>i</sub> reaches a maximum wind power of 227 watts at a 0° angle, type C<sub>ii</sub> produces a maximum wind power of 322 watts at a 4° angle, and type C<sub>iii</sub> generates a maximum wind power of 513 watts at an 8° angle. Each diffuser type reaches its peak wind power at different angles because the optimal angle for maximizing windspeed or wind power output varies depending on the length of diffuser. By increasing of wind power available, the wind energy can be significantly converted by the wind turbine so that the power output of the wind turbine can be increased

### CONCLUSIONS

From the analysis and calculations of the obtained data, it can be observed that using an airfoil on the diffuser can significantly increase wind velocity in the throat area compared to a simple diffuser. The Wortman FX63-137 airfoil, utilized on the diffuser, enhances the incoming wind velocity across various types. Increasing the length of the diffuser results in higher wind speed, but raising the angle of attack beyond a certain inclination can reduce the wind speed. For diffuser type C<sub>0</sub>, the wind velocity increases up to 6.95 m/s but drops significantly after exceeding a 2° angle. Type C<sub>i</sub> achieves its highest wind speed of 7.59 m/s at a 0° angle, with a decrease observed at subsequent angles. Type C<sub>i</sub> experiences a decline starting from 6°, while type C<sub>ii</sub> shows no decline in the graph but has the potential to decrease at larger angles. The wind power output is influenced by wind speed, with the highest power of 513 watts generated by type C<sub>iii</sub> at an angle of 8°. Conversely, the lowest wind power of 137 watts is produced by type C<sub>0</sub>, also at an 8° angle.

### ACKNOWLEDGEMENTS

I am deeply grateful to the Mechanical Engineering Department of Mataram University for providing access to the computer lab, which enabled the use of ANSYS and Autodesk Inventor, significantly contributing to the smooth progress of this research. I am also immensely thankful to Mr. I Kade Wiratama and Mr. I Wayan Joniarta for their guidance and support, which made the publication of this journal possible. Additionally, I

extend my heartfelt thanks to my friend, Baginda Arsyi Muhammad, for his invaluable assistance throughout this research.

## DECLARATION OF CONFLICTING INTERESTS

The author(s) declared no potential conflicts of interest regarding the research, authorship, or publication of this article.

## FUNDING

## REFERENCES

- [1] F.A Muhajir and N. Sinaga, "Tinjauan Pemanfaatan Energi Bayu Sebagai Pembangkit Listrik di Provinsi Sulawesi Selatan," *JURNAL TEKNIKA*, vol. 15, no. 01, pp. 55–61, Jun. 2021.
- [2] S. Bektiarso, I. K. Mahardika, N. M. Anggraeni, R. E. Kinasih, and N. A. Jannah, "Kemampuan Alat Kincir Angin Sederhana Dalam Menghasilkan Listrik," *Jurnal Ilmiah Wahana Pendidikan*, vol. 9, no. 3, pp. 488–493, Feb. 2023.
- [3] A. Fauzzy, C. D. Yue, C. C. Tu, and T. H. Lin, "Understanding the Potential of Wind Farm Exploitation in Tropical Island Countries: A Case for Indonesia," *Energies (Basel)*, vol. 14, no. 2652, pp. 1–26, May 2021.
- [4] A. Sebastiani, F. Castelani, G. Crasto, and A. Segalani, "Data Analysis and Simulation of the Lillgrund Wind Farm," *Wiley*, pp. 634–648, Nov. 2020.
- [5] Sahid, Mulyono, T. Prasetyo, D. Hendrawati, Y. M. Safaruudin, and M. F. alyasa, "Turbin Angin Poros Horizontal Tipe Flat Sudu Banyak Taper 4:5 dan Sudut Keluaran 25°," *Jurnal Rekayasa Mesin*, vol. 17, no. 1, pp. 169–178, Apr. 2022.
- [6] M. A. Rahamatian, P. H. Tari, M. Mojaddam, and S. Majidi, "Numerical and Experimental Study of the Ducted Diffuser Effect on Improving the Aerodynamic Performance of a Micro Horizontal Axis Wind Turbine," *Elsevier*, vol. 245, pp. 1–27, Apr. 2022.
- [7] B. A. J. Al-Quraishi *et al.*, "CFD Investigation of Empty Flanged Diffuser Augmented Wind Turbine," *Penerbit UTMH*, vol. 12, no. 3, pp. 22–32, 2020.
- [8] A. Susandi, F. Arifin, and R. D. Kusumanto, "Simulation of Diffuser Parameters in the Performance of Horizontal Axis Wind Turbine using Computational Fluid Dynamics," *Technology Reports of Kansai University*, vol. 63, no. 06, pp. 7739–7749, Jun. 2021.
- [9] A. Agha, H. N. Chaudry, and F. Wang, "Determining the Augmentation Ratio and Response Behaviour of a Diffuser Augmented Wind Turbine (DAWT)," *Elsevier*, vol. 37, pp. 1–32, Feb. 2020.
- [10] M. M. Naji and B. A. Jabbar, "Diffuser Augmented Wind Turbine: A Review Study," *AIP Publishing*, vol. 3051, no. 1, pp. 1–15, Feb. 2024.
- [11] A. Alanis, J. A. Franco, S. Piedra, and J. C. Jauregui, "A novel high performance diffuser design for small DAWT's by using a blunt trailing edge airfoil," *Techno Press*, vol. 32, no. 1, pp. 1–7, Jan. 2020.
- [12] A. M. Elyased, "Design Optimization of Diffuser Augmented Wind Turbine," *Akademia Baru*, vol. 13, no. 8, pp. 45–59, Aug. 2021.
- [13] I. K. Wiratama, I. M. Suartika, I. W. Joniarti, I. M. Mara, I. M. Nuarsa, and M. Ansori, "Analysis Aerodynamic Performance Airfoil WORTMANN FX63-137 in Different Reynolds Number," *Atlantis Press*, pp. 125–31, Dec. 2022.

- [14] M. H. G. Syafei, R. T. Indrawati, and T. A. Farhan, "Implementation of the Airfoil parameterization PARSEC Method in Python," *Jurnal Rekayasa Mesin*, vol. 17, no. 3, pp. 485–494, Dec. 2022.
- [15] Y. Ohya and T. Karasaduni, "A Shrouded Wind Turbine Generating High Output Power with Wind-lens Technology," *Energies (Basel)*, vol. 3, no. 4, pp. 634–649, Mar. 2010.
- [16] T. Matsushima, S. Takagi, and S. Muroyama, "Characteristics of a highly efficient propeller type small wind turbine with a diffuser," *Elsevier*, vol. 31, no. 9, pp. 1343–1354, Jul. 2006.
- [17] M. M. Darpe, S. K. Bandekar, and S. V. Panjari, "Design and Optimization of a Diffuser Augmented Wind Turbine (Wind Lens Turbine) using CFD," *International Research Journal of Engineering and Technology (IRJET)*, vol. 7, no. 4, pp. 962–968, Apr. 2020.
- [18] K. Watanabe and Y. Ohya, "A Simple Theory and Performance Prediction for a Shrouded Wind Turbine with a Brimmed Diffuser," *Energies (Basel)*, vol. 14, no. 3661, pp. 1–15, Jun. 2021.
- [19] Y. P. Andriyani and A. K. Munashta, "Analisis Potensi Dan Pemetaan Teknologi Turbin Angin Di Seluruh Indonesia," *Analisis Potensi dan Pemetaan Teknologi Turbin Angin di Seluruh Indonesia*, vol. 3, no. 2, pp. 77–82, 2022.
- [20] E. E. Ambarita, Harinaldi, R. Azhari, and R. Irwansyah, "Experimental study on the optimum design of diffuser augmented horizontal-axis tidal turbine," *Clean Energy*, vol. 6, no. 5, pp. 776–786, Nov. 2022.
- [21] F. Arifin et al., "Modelling Design Diffuser Horizontal Axis Wind Turbine," *Atlantis Press*, vol. 9, pp. 193–196, 2021.
- [22] Michael S. Selig and Bryan D. McGranahan, "Wind Tunnel Aerodynamic Tests of Six Airfoils for Use on Small Wind Turbines," Urbana, Oct. 2004.
- [23] M. R. Nur, "Pengembangan Model Diffuser Pada Berbagai Tinggi Flange Dengan Metode Komputasi Ansys," *Energi*, Universitas Mataram, Mataram, 2022.
- [24] Sudarma A F and Widiyanto F, "Studi Numerik Pengaruh Geometri Supply Air Grille serta Variasi Kecepatan Udara Masuk Terhadap Distribusi Temperatur di Dalam Ruangan Terkondisi," *Jurnal Teknik Mesin*, vol. 10, no. 1, pp. 27–37, Feb. 2021.
- [25] L. E. N. Putra, S. Sugeng, M. Ridwan, A. Widyandari, and A. K. Yusim, "Analisis Performa Heat Transfer pada Plastic Welding terhadap Sambungan Pelat Perahu Berbahan High Density Polyethylene (HDPE) Menggunakan Finite Element Method," *Jurnal Rekayasa Mesin*, vol. 19, no. 3, pp. 419–430, Dec. 2024.
- [26] Prasetiyo A B, fauzun, Azmi A A, Pamuji D S, and Yaqin R I, "Pengaruh Perbedaan Mesh Terstruktur dan Mesh Tidak Terstruktur Pada Simulasi Sistem Pendinginan Mold Injeksi Produk Plastik," *Prosiding Nasional Rekayasa Teknologi Industri dan Informasi*, pp. 400–406, Nov. 2018.
- [27] Hutaauruk R M, "Simulasi numerik tahanan kapal gillnet menggunakan pendekatan computaional fluids dynamics," *Jurnal Perikanan dan Kelautan*, vol. 4, pp. 35–47, Jun. 2013.
- [28] R. F. Billad, J. Julian, F. Wahyuni, and W. Iskandar, "Numerical Modelling of NACA 0015 Airfoil Under Erosion Condition," *Jurnal Rekayasa Mesin*, vol. 19, no. 2, pp. 199–210, Aug. 2024.

- [29] M. S. Hasan and Widayat, "Produksi Hidrogen dengan Memanfaatkan Sumber Daya Energi Surya dan Angin di Indonesia," *JEBT: Jurnal Energi Baru & Terbarukan*, vol. 3, no. 1, pp. 38–48, Apr. 2022.
- [30] Ridzuan F, Omar M H, Didane D H, Manshoor B, Abdelaal M A, and Amin A, "Aerodynamic Performance of NACA S809 Wind Turbine Blade Airfoil Using SST K-omega and K-epsilon Turbulence Models," *Journal of Design for Sustainable and Environment*, vol. 6, no. 2, pp. 36–42, Aug. 2024.